Two Basic Problems for Hot Dry Rock Reservoir Stimulation and Production

Xi Zhang, Rob Jeffrey*, and Bisheng Wu
CSIRO Petroleum Resources, Melbourne, Australia
*Tel: 03-95458354, E-mail: rob.jeffrey@csiro.au

A numerical analysis is made for heat extraction from a geothermal reservoir in a naturally fractured rock mass. We consider in particular two issues: long-term prediction of fluid temperature around a single fracture and the initial stages of fracture development in a naturally fractured rock. For the first problem, the evolution of outlet fluid temperature is considered as a function of time and injection rate. The rock temperature around a single fracture in the reservoirs is also calculated. The second problem is motivated by the fact that injection pressure is highly dependent on the details of fracture geometry near the borehole. High treatment pressure are associated with the formation of opening mode hydraulic fractures in naturally fractured rock and recent result that can explain the origin of these pressures are applied here to the problem of high injection impedance at pressures below the jacking pressure.

Keywords: Hot Dry Rock, fluid flow, thermal effect, crack growth, numerical method

Introduction

In stimulation and operation of an Enhanced Geothermal System (EGS), fluid circulation is influenced in both the short and long-term by thermal-hydro-mechanical deformation. In other words, the efficiency for hot-dry-rock reservoir stimulation and production depends on fracture interconnectivity and thermal flux interchanges between rock and fluid coupled to fracture permeability (Bodvarsson, 1969; Hallow and Pracht, 1972; Gringarten, et al., 1975; Abe et al., 1976; Cheng et al., 2001). We present results from two problems that, at this point, include limited coupling. The first problem involves calculation of the evolution of heat transfer between rock and fluid over a long period of time and the second problem considers the effect of pre-existing fracture interconnectivity along a non-planar path on injected fluid pressure and crack growth. Both problems are useful in demonstrating the importance of coupled processes, e.g., thermal-hydraulic coupling for the first problem and hydraulic and mechanical deformation coupling for the second problem. We are working towards a thermal-hydraulic-mechanical coupled analysis of both problems.

We first address the interaction between the long-term heat extraction and fluid flow and heat conduction in both rock and fluid. The cooling of rock around an axisymmetric reservoir containing a single conductive fracture is discussed. In the second part of this paper we give a detailed study on how a fracture propagates through a fracture network that guides its path. The spatially varying fracture conductivity that results from stress-dependent fracture permeability has a strong effect on the fluid pressure distribution. As a result, the injection pressure is found to be elevated.

Thermal Analysis of Penny-Shaped Fracture Reservoirs

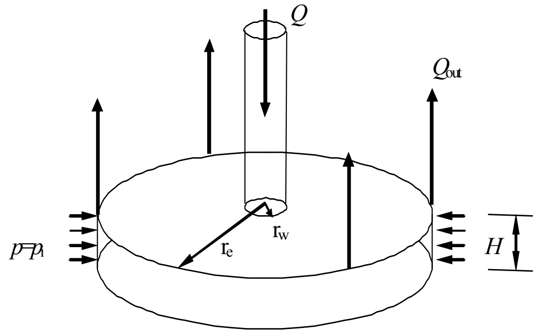

Figure 1: An axisymmetric penny-shaped geothermal reservoir.

Fracture conductivity and fluid flow

For a large naturally fractured geothermal reservoir, Pine and Batchelor (1984) found that the fracturing during injection was dominated by shear and associated dilation. For simplicity, shear deformation caused by far-field stresses interacting with the injected fluid pressure is not considered in this simple thermal-fluid model presented here and the reservoir is considered to consist of a impermeable layer of a finite thickness *H*, as shown in Fig.1. The reservoir layer is assumed to axisymmetric, with production wells located at the periphery of a circle with a radius r_e. The conductivity between the injection and production wells is provided by a single conductive fracture located at the midplane of the reservoir for the analysis of fluid flow and heat conduction. Practically, this closed but conductive fracture model, which uses an effective hydraulic aperture (<1 mm in most cases) held constant along its extent, is useful in studying the thermal-fluid system. The fracture aperture, in real natural fractures, has been shown to vary along the fracture with, surface roughness, effective stress, temperature and chemical processes (Min, et al., 2008). The fracture conductivity then is modelled by the cubic law with the fracture permeability given as follows (Tsang and Witherspoon, 1981)

$$k = \frac{w_0^{\ 2}}{12} \tag{1}$$

where k is the fracture permeability and w_0 is the effective hydraulic aperture for the closed natural fracture. We assume that the small roughness present and induced changes in the hydraulic aperture along the natural fracture can be ignored because the aperture change occurs with a small slope so that the cubic law is still valid (Brown et al. 1995).

Darcy's law is used to describe fluid flux in response to fluid pressure gradient ∇p_f

$$q_f = -\frac{k}{\mu}\nabla p_f \tag{2}$$

where μ is the fluid dynamic viscosity.

Problem statement

As shown in Fig. 1, a fluid (at temperature T_i) is injected into the reservoir at a constant rate Q. The production wells are assumed to be uniformly distributed along the periphery of the reservoir with a constant production pressure p_o, so that the fluid flow and temperature change distributions are axisymmetric. The reservoir height is *H,* which also represents the spacing between conductive fractures in the reservoir or the designed fracture interval.

Based on fluid mass continuity, the governing equation for pressure diffusion in the axisymmetric fracture is given by

$$\frac{\partial p_f}{\partial t} = c\left(\frac{\partial^2 p_f}{\partial r^2} + \frac{1}{r}\frac{\partial p_f}{\partial r}\right) \tag{3}$$

where $c = k/\chi\mu$ and χ is the elastic pore compressibility.

The solution to the above equation at given boundary and initial conditions can be found in the monograph by Carslaw and Jaeger (1959).

Let q_h denote the heat flux from rock to fluid at the fracture surface. Based on previous studies (Abe et al., 1983; Cheng, et al., 2001), the heat dissipation and storage along the fracture can be neglected. For the axisymmetric problem posed above, the heat transfer equation along the fracture surface can be written as (Abe et al., 1983; Cheng, et al., 2001)

$$\rho_w c_w q_f \cdot \frac{\partial T_f}{\partial r} + q_h = 0 \tag{4}$$

where T_f is the temperature along the fracture, and ρ_w and c_w are the mass density and specific heat of the fluid.

In the presence of heat exchange between rock and fluid, the rock temperature will vary in the form of

$$T_r = T_\infty + \frac{2}{\sqrt{\pi}}\int_0^t \frac{1}{[4\kappa_r(t-t')]^{3/2}}\int_{r_w}^{r_e} q_h I_0\left(\frac{rr'}{2\kappa_r(t-t')}\right) \exp\left(-\frac{r^2+r'^2+z^2}{4\kappa_r(t-t')}\right) r'dr'dt' \tag{5}$$

where T_∞ is the initial uniform temperature of the rock, the rock thermal diffusivity is $\kappa_r = K_r/(\rho_r c_r)$ in which K_r is the rock thermal conductivity, and ρ_r and c_r are the mass density and specific heat of the rock. Finally, I_0 is the modified Bessel function of the first type.

Based on the continuity of temperature across the fracture surface, the governing equation for temperature change can be established by considering the equivalence of fluid temperature calculated by Eq. (4) and the rock temperature at the fracture surface by Eq. (5). This leads to an integral equation, which can be solved numerically by the collocation method. Moreover, the corresponding initial and boundary conditions are not listed here to save space.

Numerical results

As an example, we consider the case of reservoir radius r_e=300 m and wellbore radius r_w=0.1 m, and initial rock temperature of 270°C (or 543 K). Water with a constant viscosity μ=0.0004 Pa·s, although we recognise that the viscosity will depend on temperature, is injected into the fracture at a constant rate *Q*=20 l/s and at an initial temperature of 70°C (or 343 K). The reservoir height or thickness is H=0.5 m. The fracture hydraulic aperture w_0 is 1 mm. The rock thermal conductivity K_r=2.4 W/m·K, and the rock mass density and heat capacity are ρ_r=2700 kg/m^3 and c_r=1000 J/kg·K, respectively. The fluid temperature at the outlet is plotted against elapsed time in Fig. 2 and the temperature contours in the rock, at 1.92 and 14.26 years after the start of injection, are shown in Fig. 3.

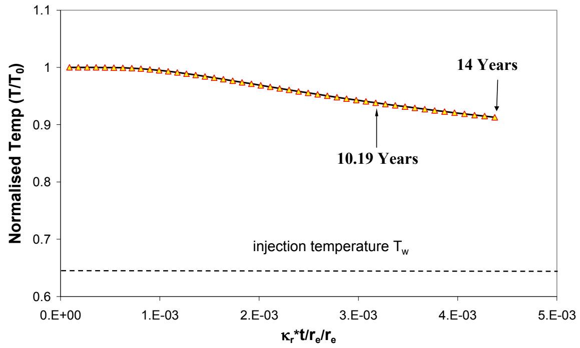

Figure 2 Normalised fluid temperature at production well against time

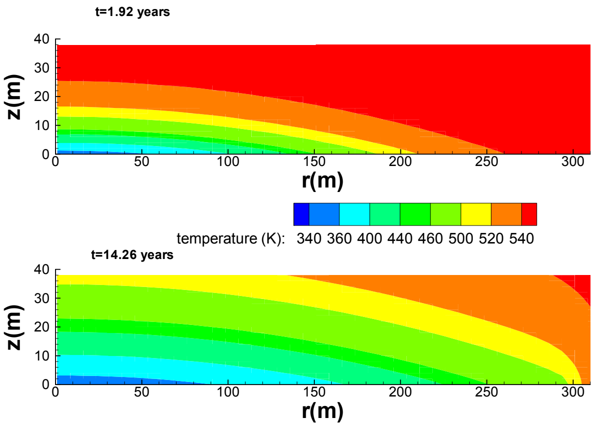

Figure 3 Temperature contours in the reservoir rock between the injection and production wells. The production well is at r=300 m.

Fracture Growth along an Offset Natural Fracture

As the geothermal reservoir is comprised of naturally fractured rock, the injected fluid will more or less follow the path defined by existing conductive fractures. In particular, injected water may reach a pressure sufficient to open some portions of natural fractures near the injection wellbore. The fluid flow is guided by the conductive channels and analysis of this problem involves tracking the strong coupling between rock deformation and fluid flow. The induced near-bore inflow restriction can limit fluid production eventually. To start, we idealise the fracture geometry as shown in Fig. 4. We consider the pressure and crack opening responses when injection is located at the start of a natural fracture that contains several offsets along its path (Fig. 4). The fracture geometry including the step and offset sizes and their intersection angle θ are shown in the figure, along with the far-field stresses and material constants used. The closed natural fracture is assumed to be conductive with an initial hydraulic aperture w_0. In this section, w_0 is 0.01 mm for all cases, unless otherwise specified. Although the real situation results in a 3D problem, it is here treated as a plane strain problem instead.

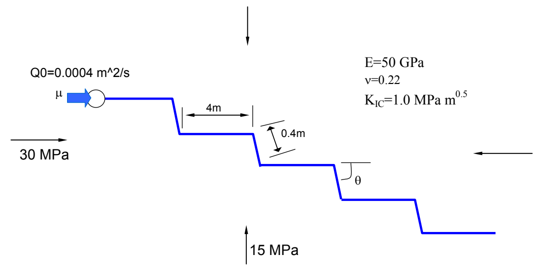

Figure 4 Schematic of an offset natural fracture with fluid injected at one end. K_{IC} is the fracture toughness of the rock.

Fracture slip model

Fracture frictional slip along parts of the fracture can be important in this case since there is a strong horizontal compressive far-field stress. We use the Coulomb frictional law, which is applied locally to the cohesionless, but frictional fracture, to provide a limit on the frictional stress τ_s in terms of the normal effective compressive stress, $\sigma_n - p_f$,

$$|\tau_s| \le \lambda(\sigma_n - p_f) \tag{6}$$

where λ is the coefficient of friction and $\lambda(\sigma_n - p_f)$ is the frictional strength. For the dry portion of the fracture $p_f = 0$. In this paper, λ =0.8 for all cases.

Hydraulic fracturing model

As fractures can be opened by fluid pressure, elastic deformation associated with fluid flow must be considered here. The governing equation for fracture equilibrium is given as follows in the presence of multiple cracks,

$$\sigma_n(\boldsymbol{x},t) - \sigma_1(\boldsymbol{x}) = \sum_{r=1}^{N}\int_0^{l_r}[G_{11}(\boldsymbol{x},s)w(s) + G_{12}(\boldsymbol{x},s)v(s)]\mathrm{d}s \tag{7}$$

$$\tau_s(\boldsymbol{x},t) - \tau_1(\boldsymbol{x}) = \sum_{r=1}^{N}\int_0^{l_r}[G_{21}(\boldsymbol{x},s)w(s) + G_{22}(\boldsymbol{x},s)v(s)]\mathrm{d}s \tag{8}$$

where N is the number of cracks, $G_{\alpha\beta}$ $(\alpha, \beta$ =1,2) are Green's functions, w, v are opening and shearing displacement discontinuities across the fracture surface, and σ_1, τ_1 are the normal and shear stresses, respectively, acting along the fracture direction at location $\boldsymbol{x}$ generated by the far-field stresses.

In the existence of fracture opening (hydraulic fracturing), the fluid flow along the fracture can be described by Reynolds' equation as follows (Batchelor, 1967)

$$\frac{\partial(w+\varpi)}{\partial t}=\frac{\partial}{\partial s}[\frac{(w+\varpi)^3}{\mu'}\frac{\partial P_f}{\partial s}] \qquad (9)$$

where $\mu'=12\mu$. It should be noted that the total hydraulic opening is the sum of fracture mechanical opening and initial hydraulic aperture ϖ. Furthermore, the hydraulic aperture can vary with the effective stress in the closed fracture based on a liner spring model, that is,

$$d\varpi / dp_f = \gamma\varpi \qquad (10)$$

in which γ is a small constant for characterizing the compliance of a natural fracture with respect to pressure change (1/Pa), and is assumed to be less than 10^{-8} /Pa for most cases.

The above system of equations provides all governing equations for hydraulic fracture growth. The required initial and boundary conditions are not given here and the reader can refer to our previous work for more details (Zhang et al, 2008; Zhang and Jeffrey, 2008).

Numerical results

For the case that water is used as injection fluid, the fracture opening along the offset fracture is shown in Fig. 5, at a time when the fluid just reaches the fracture tip. It is clear that there is a narrow channel at the offset locations. An increase in the offset angle results in a narrower opening in this portion of the fracture (Fig. 5).

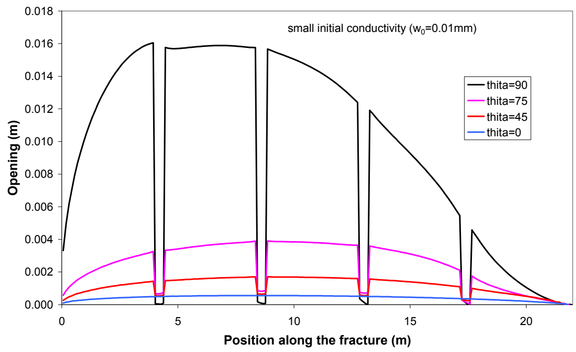

Figure 5 Fracture opening along the offset natural fracture when a hydraulic fracture is growing along it.

Figure 6 shows the time-dependent variation of the injection pressure for the offset natural fracture. Although the pressure decreases smoothly in time for a hydraulic fracture and for opening of a natural fracture without offset, it oscillates at an elevated level in the case of offset natural fractures. This reflects the different resistance for fluid flow along steps and offsets. When the fluid propagates along the steps, it will move at a lower pressure gradient. This results in pressure decreasing with time, in contrast to the increase in pressure occurring when flow is through the narrow offsets, which have lower opening compliance and are subjected to higher confining stresses.

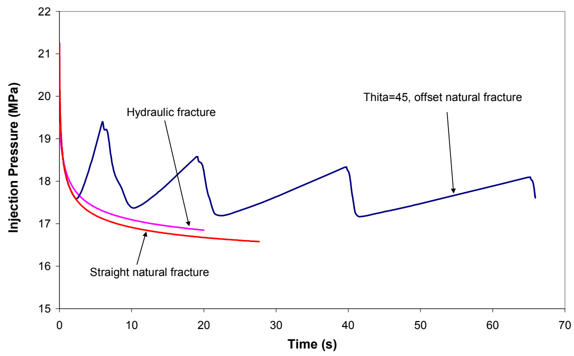

Figure 6 Pressure at the borehole against time corresponding to the cases shown in Fig. 5.

The effect of narrow offsets on the injection pressure, at pressures below the opening pressure, can be seen in Fig. 7 where the fluid is injected into the fracture at a very low injection rate Q_0=1E-7 m^2/s. The initial hydraulic aperture w_0 of the steps is increased to 0.05 mm to account for the relatively lower confining stress acting across them. Fig. 7 shows the variation of injection pressure against time when the kink angle is 45 degree. Even though the injected fluid pressure is below the confining stress so that no fracture opening occurs, a pressure increase is evident when the fluid front crosses the narrow offset region. Near-wellbore injection impedance may partly result from the injected fluid flowing along such tortuous pathways.

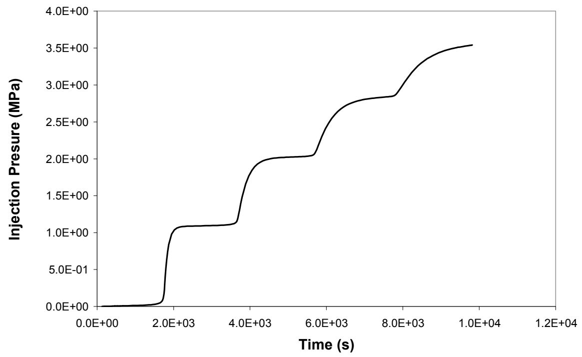

Figure 7 Pressure at the borehole against time in the case of low injection rate.

Summary and Discussion

We have presented numerical results for two basic problems, which are associated with the thermal-fluid coupling and fluid-mechanical coupling problems that arise in predicting temperature and fluid flow through a naturally fractured hot rock reservoir. From the analyses, the coupling between different mechanisms plays an important role in correctly predicting the temperature and fluid pressure changes. We intend to next implement thermoelastic coupling in the 2D model used above.

In the first model, we have not considered the effect of elastic deformation. As we know, shear deformation assisted by surface roughness can induce fracture shear-induced dilatation that increases the fracture conductivity. Also, the reduction in effective stress caused by fluid pressure and the thermoelastic deformation resulting from cooling of rock can increase the fracture permeability. Chemo-mechanical processes should also be considered. These effects have been studied by coupled reservoir models (Min et al., 2008). Our approach is to extend our 2D hydraulic fracture model to include thermoelastic effects and apply it to the coupled mechanics of complex fracture geometries to analyse mechanism leading to local near-wellbore elevation of injection impedance. The results of this detailed mechanical modelling can then be incorporated in a more simplified way into reservoir-scale models.

References

Abe, H., Mura, T., and Keer, L. M., 1976, Growth rate of a penny-shaped crack in hydraulic fracturing of rocks, J. Geophysical Research vol 81, p5335-5340.

Abe, H., Sekine, H. and Shibuya, Y., 1983, Thermoelastic analysis of cracklike reservoir in a hot dry reock during extraction of geothermal energy, J of Energy Resources Technology vol 105, p503-508.

Batchelor, G.K., 1967, An Introduction to Fluid Dynamics, Cambridge University Press, Cambridge, U.K.

Bodvarsson, G., 1969, On the temperature of water flowing through fractures', J Geophysical Research vol 74, p1987-1992.

Brown, S. R., Stockman, H. W. and Reeves, S. J., 1995 Applicability of the Reynolds equation for modelling fluid flow between rough surfaces, Geophysical Research Letter vol 22, p2537-2540.

Carslaw, H. S. and Jaeger, J. C. 1959, Conduction of heat in solids, Oxford University Press, Oxford, U. K.

Cheng, A. H.-D., Ghassemi, A. and Detournay, E., 2001, Integral equation solution of heat extraction from a fracture in hot dry rock, Int. J. for Numerical and Analytical Methods in Geomechanics vol 25, p1327-1338.

Gringarten, A. C., Witherspoon, P. A. and Ohnishi, Y., 1975 Theory of heat extraction from fractured hot dry rock, J. Geophysical Research 80, p1120-1124.

Hallow, F. H. and Pracht, W. E. 1972 A theoretical study of geothermal energy extraction, J. Geophysical Research vol. 77, p7038-7048.

Min, K.-B., Rutqvist, R., and Elsworth, D., 2008, Chemically and mechanically mediated influences on the transport and mechanical characteristics of rock fractures, International Journal of Rock mechanics and Mining Science vol. 46, p80-89.

Pine, R.J. & Batchelor, A.S., 1984, Downward migration of shearing in jointed rock during hydraulic injections, International Journal of Rock mechanics and Mining Science and Geomechanics Abstract vol. 21, p249–263.

Tsang, Y. W. and Witherspoon P. A., 1981, Hydromechanical behavior of a deformable rock fracture subject to normal stress, Journal of Geophysical Research vol. 86, p9287-9298.

Zhang, X. Jeffrey, R. G. and Thiercelin, M., 2008, Escape of fluid-driven joints from bedding interfaces: A numerical study, J. Structural Geology vol. 30, p478-490.

Zhang, X. and Jeffrey, R. G., 2008, Re-initiation or termination of fluid-driven fractures at frictional bedding interfaces, J. Geophysical Research vol 113, B08416.